Modeling Alternatives for Cerebral Carbon-11-Iomazenil Kinetics

Alfred Buck, Gerrit Westera, Gustav K. vonSchulthess and Cyrill Burger
Division of Nuclear Medicine, Department of Radiology, University Hospital, Zurich, Switzerland

The in vivo binding kinetics of [^{11}C]iomazenil, a central benzodiazepine antagonist, were analyzed using PET and compartmental modeling. This method is of interest because it allows validation of the SPECT tracer [^{123}I]iomazenil. **Methods:** The experimental protocol consisted of serial PET imaging following a single bolus injection of the radioligand. Imaging was performed on five healthy young volunteers over 106 min. The tissue time-activity curves of various brain regions were analyzed with models consisting of two (K1, k2″) and three (K1, k2′, k3′, k4) compartments. Some of the methods use simultaneous fitting of the data from multiple brain regions coupled with common parameters. Distribution volumes and k3-based parameters [(K1/k2′) k3′ and k3′)] were chosen to represent receptor density. Goodness of fit was assessed with F-test statistics and chi-square analysis. **Results:** Compared with the two-compartment model, goodness of fit was significantly improved by all three-compartment configurations. Of the three-compartment models, goodness of fit was similar for the configurations with K1/k2′, k4 or no parameter coupled, and slightly worse when both parameters were coupled. The most reliable estimates of receptor density were obtained from the specific distribution volumes (DVs) calculated with the three-compartment model, and the coupling of k4 or both k4 and K1/k2′. Due to oversimplification of the kinetics, the DV values calculated with the two-compartment model were underestimated. **Conclusion:** Reliable quantitative information regarding benzodiazepine receptor density following bolus injection of iomazenil is best obtained by tracer kinetic modeling that uses a three-compartment model and parameter coupling.

Key Words: carbon-11-iomazenil; benzodiazepine receptors; PET; kinetic modeling

J Nucl Med 1996; 37:699–705

Changes in central benzodiazepine receptor density have been reported in various neurologic disorders such as epilepsy (*1–6*) and neurodegenerative diseases. Until recently, the quantitative in vivo assessment of neuroreceptor status required PET. A suitable PET ligand for benzodiazepine receptors is [^{11}C]-flumazenil and its binding kinetics have been evaluated by different groups extensively (*7–9*). It appears that quantitative evaluation of neuroreceptors is also possible with the less expensive and more widely available latest generation of SPECT cameras. The methods formerly restricted to PET have been successfully applied to the evaluation of the binding kinetics of [^{123}I]-iomazenil measured with SPECT in animals (*10,11*) and in humans (*12*). Since PET is still the gold standard in quantitative imaging, however, analogous SPECT procedures have to be carefully validated. To allow a direct PET-SPECT comparison, we labeled iomazenil with ^{11}C and ^{123}I and performed binding studies with both modalities in a group of healthy young volunteers. The purpose of this part of the study was to evaluate different receptor related parameters derived from two- and three-compartment models for the quantitation of [^{11}C]iomazenil benzodiazepine receptor binding with PET. Some of the methods use simultaneous fitting of the data from multiple brain regions in conjunction with coupled parameters. This approach was successfully applied to cardiac ^{11}C-acetate studies by Raylman et al. (*13*).

Received Jan. 30, 1995; revision accepted Aug. 18, 1995.
For correspondence or reprints contact: Alfred Buck, MD, Division of Nuclear Medicine, Department of Radiology, University Hospital, 8091 Zurich, Switzerland.

MATERIALS AND METHODS

Theory

The following derivations follow the work by Koeppe et al. (*9*). Compartmental modeling of receptor ligand usually starts with model as shown in Figure 1, which consists of four compartments corresponding to extractable ligand in arterial plasma (Cp), free ligand in tissue (Cf), ligand bound nonspecifically (Cns) and specifically (Cs). The following six rate constants describe the exchange of ligand between the different compartments:

$$K1 = CBF \times E\ [ml\ g^{-1}\ min^{-1}] \quad \text{Eq. 1}$$

$$k3 = kon\ Bmax\ [min^{-1}] \quad \text{Eq. 2}$$

$$k4 = koff\ [min^{-1}] \quad \text{Eq. 3}$$

$$Kd = koff/kon \quad \text{Eq. 4}$$

$$k3/k4 = Bmax/Kd, \quad \text{Eq. 5}$$

where K1 = blood-to-brain transport of ligand, CBF = mass specific blood flow (ml g^{-1} min^{-1}), E = first-pass extraction fraction, kon = bimolecular association rate between ligand and receptor, Bmax = density of unoccupied receptors, koff = dissociation rate of ligand from receptors, and Kd = equilibrium binding constant for specific receptor sites. When there is rapid equilibration between the free and nonspecific compartment, model a can be reduced to model b.

The following relationships exist between the rate constants of models a and b:

$$k2' = k2/(1 + k5/k6) = K1/DV' = K1/DVf(1 + k5/k6)$$
$$= K1/DVf + ns \quad \text{Eq. 6}$$

$$k3' = k3/(1 + k5/k6) = kon\ Bmax/(1 + k5/k6), \quad \text{Eq. 7}$$

where DV′ = DVf(1 + k5/k6) = DVf+ns is the summed distribution volume of the free and nonspecifically bound ligand.

The distribution volume (DVs) of the specifically bound ligand is defined as:

$$DVs = (K1/k2')\ (k3'/k4). \quad \text{Eq. 8}$$

As described by Mintun et al. (*14*), DVs can be expressed in terms of the binding potential (BP = Bmax/Kd):

$$DVs = (K1/k2')\ (k3'/k4) = K1/k2\ k3/k4$$
$$= K1/k2\ Bmax\ kon/koff = K1/k2\ BP. \quad \text{Eq. 9}$$

Assuming passive diffusion of iomazenil across the blood-brain barrier, K1 is equal to k2 if no protein binding occurs in the plasma.

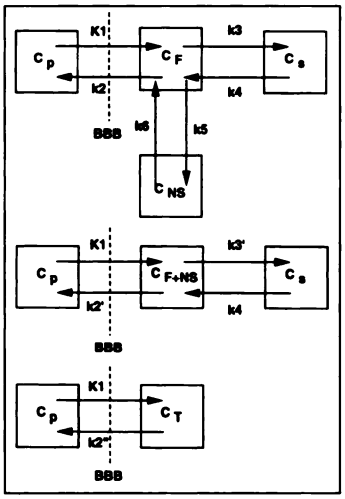

FIGURE 1. Model configurations for the assessment of [^{11}C]iomazenil binding to benzodiazepine receptors. Cp = free ligand in plasma tissue, CF = free ligand in tissue, CNS = nonspecifically bound ligand, Cs = specifically bound ligand and BBB = blood-brain barrier.

With protein binding, K1/k2 represents the fraction of free ligand in plasma (f1) when the total ligand in plasma (free plus protein-bound) is taken as the input curve:

$$K1/k2 = f1, \text{ or } k2 = K1/f1 \qquad \text{Eq. 10}$$

The combination of Equations 9 and 10 yields the following relationship between DVs and BP

$$DVs = f\,BP \qquad \text{Eq. 11}$$

Another potentially useful parameter related to receptor density is (K1/k2′) k3′. Inserting k2 and k3 from Equations 6 and 7 yields the following relation:

$$(K1/k2')\,k3' = (K1/k2)\,k3 = (K1/k2)\,Bmax\,kon$$

or, considering Equation 10:

$$(K1/k2')\,k3' = f1\,Bmax\,kon. \qquad \text{Eq. 12}$$

Moreover, if there is rapid equilibration between the two tissue compartments of model b and model a, further reduction to model c is possible.

$$k2'' = k2'/(1 + k3'/k4) = k2/[(1 + k5/k6)/(1 + k3'/k4)]$$

$$= k2/(1 + k5/k6 + k3/k4) = K1/DV'',$$

where DV″ = K1/k2″ = DVf + DVns + DVsp is the total distribution volume of ligand in tissue.

Chemistry

Carbon-11-iomazenil was prepared as previously described (*15*). Briefly, [^{11}C]methyliodide ([^{11}C]-MeI) was prepared from [^{11}C]-CO_2 by reduction with $LiAlH_4$ in dry THF and, after removal of the THF, subsequent reaction with HI. The [^{11}C]-MeI was reacted with demethyl-iomazenil in 200 μl DMF with NaH for 2 min at 70°. The [^{11}C]MeI was purified by HPLC over Nucleosil-C18, 10 μ, 250 × 8 mm (Knauer) eluting with 65 m*M* H_3PO_4/acetonitrile (69/31).

Chemical and radiochemical purity and specific activity were assayed by analytical HPLC with 65 m*M* H_3PO_4/acetonitrile (60/40) over Nucleosil-C18, 10 μ, 250 × 4 mm. The amount of iomazenil carrier was determined by comparing the UV signal with a standard value.

Subjects

Five healthy university students (aged 20–23 yr) were recruited for participation in the study. None had a history of psychiatric or neurological disorders or drug abuse. Informed consent was obtained from all patients and the study was approved by University Hospital.

PET

PET imaging was performed on a scanner with 7–8 mm reconstructed resolution. Data from four rings were acquired simultaneously, thereby allowing the reconstruction of seven planes with a slice-to-slice separation of 8 mm.

Head motion during scanning was restricted by the use of an individually fitted polyurethane mold. After placement of a radial artery and cubital vein catheter, the subjects were positioned supine in the scanner with their eyes and ears unoccluded. Before radioligand injection, a 10-min transmission scan was obtained to correct for attenuation. Scanning was performed parallel to the orbitomeatal line with a field of view of 5.6 cm. The inferior border was positioned 3 cm above the orbitomeatal line. After intravenous injection of 111–222 MBq (3–6 mCi) [^{11}C]iomazenil as a slow bolus over 4.5 min with an infusion pump, dynamic PET scans were obtained: four 1-min, three 2-min, three 7-min, five 10-min and one 15-min.

Timed arterial blood samples were withdrawn into heparinized syringes every 30 sec for the first 6 min, followed by progressively longer time intervals until the end of the scanning period.

Blood and Plasma Analysis

Blood samples at 1, 2, 3, 4, 5, 6, 8, 10, 14, 20, 30, 40, 60, 75 and 90 min were analyzed for metabolites using chloroform separation. After centrifugation, 0.5 ml plasma was added to an equal volume of borate buffer (0.1 *M* H_3BO_3/NaOH, 0.05 *M* KCl, pH = 11) and 1 ml chloroform. After vortexing for longer than 1 min, the sample was centrifuged for 7 min at high speed at 15°–20°, after which a 0.5-ml water layer and a 0.5-ml chloroform layer were pipetted and counted. At the chloroform-water boundary, a solid phase of denatured protein was found in the chloroform layer which was also counted in three cases. The amount of nonextractable protein-bound radioactivity was also calculated by subtracting the activity in the water and chloroform layers from the total activity counted in the plasma layer.

The radioactivity in the chloroform layer represented the amount of authentic plasma iomazenil Cp and was confirmed by HPLC analysis (Nucleosil-C18, 10 μ, 250 × 4 mm, eluting with 65 mmole H_3PO_4/acetonitril [60/40]) of the chloroform and water layers of the 5- and 10-min samples (*12*). An on-line high sensitivity radioactivity detector was used in series with a UV detector.

Data Analysis

The plasma data (well counter units, cpm) were expressed in scanner units by doing a calibration measurement using a 20-cm cylindrical phantom.

Emission data were then attenuation-corrected and reconstructed on a 128 × 128 matrix using filtered backprojection (Hanning filter), which yielded seven transaxial slices with a slice-to-slice separation of 8-mm.

Regions of interest (ROIs) were defined over the occipital, frontal, lateral, temporal and cerebellar cortices, the striatum; thalamus and pons, and the corresponding tissue time-activity curves were calculated.

Five different model configurations were implemented for analysis of the regional iomazenil kinetics. The most simple configuration was the two-compartment model (model c), while the most complex was the three-compartment model (model b). The other three configurations were based on the three-compartment model with different combinations of parameter constraints. The different methods are summarized in Table 1. In methods B, C and D, the value of the coupled parameters was determined by fitting model b to the data of all regions, with the exception of pons, with the condition that the coupled parameters be the same for all the regions. Data from the pons were not included because of noise.

TABLE 1
Fitting Strategies

Method	No. of compartments	Model	Coupled parameters	Receptor-related outcome measures
A	2	c	None	DV″
B	3	b	K1/k2′, k4	DVs, K1/k2′ × k3′, k3′
C	3	b	K1/k2′	DVs, K1/k2′ × k3′, k3′
D	3	b	k4	DVs, K1/k2′ × k3′, k3′
E	3	b	None	DVs, K1/k2′ × k3′, k3′

The parameter values for the pons were then separately calculated with the coupled parameters that were fixed to the values calculated with the fit to other regions. Since the total activity measured in a region is composed of counts from tissue and blood, all models contained a parameter (α) to correct for blood activity:

$$CROI = (1 - \alpha)\, CT + \alpha\, Cblood,$$

where CROI = PET counts in a ROI, α = the percentage of intravascular space in tissue, CT = iomazenil counts in the extravascular compartment and Cblood = total blood activity. Parameter α was fixed to 5%.

Measures for Receptor Density

In the two-compartment model, the total distribution volume (DV″) was considered an acceptable measure for receptor density if specific binding was high compared to nonspecific binding. In the three-compartment model, the distribution volume of the specific compartment (DVs), parameter k3′ and the combination K1/k2′ × k3′ were calculated. DVs is closely related to the binding potential shown in Equation 11. Parameter k3′ will be a good measure of kon Bmax if there is not much variation in nonspecific binding (e.g., k5/k6 is relatively constant, Equation 7). Parameter K1/k2′ × k3′ is directly proportional to konBmax if the fraction of free iomazenil in plasma is relatively stable (Eq. 12).

Assessment of Methods

Several criteria were used to assess the quality of the methods.

Goodness-of-fit. The goodness-of-fit of the different models was compared using F-test statistics and chi-square analysis.

Identifiability of the Kinetic Parameters for Full Study Duration. The identifiability of the parameter estimates was assessed by means of a Monte Carlo simulation. For each model and ROI, simulated time-activity curves were generated by adding pseudo-Gaussian noise with a s.d. of 10% to the model-predicted values of the time-activity curves at the time-points of the scans. These simulated curves were then refitted with the corresponding model. The coefficient of variation (s.d./mean) from 60 runs was taken as a measure of identifiability. Another measure for stability is the coefficient of variation among the five subjects.

Sometimes the diagonal of the covariance matrix is used as a measure for identifiability. Limitations of this method include the fact that the values represent a linear approximation to an inherently nonlinear problem, and that combinations of parameters cannot be evaluated. These limitations, however, are avoided by the Monte Carlo simulation.

Stability of the Kinetic Parameters Versus Study Duration. For methods A and E (two- and three-compartment models with no parameter constraints) the stability of the parameters as a function of study duration was estimated by consecutively shortening the fitting interval.

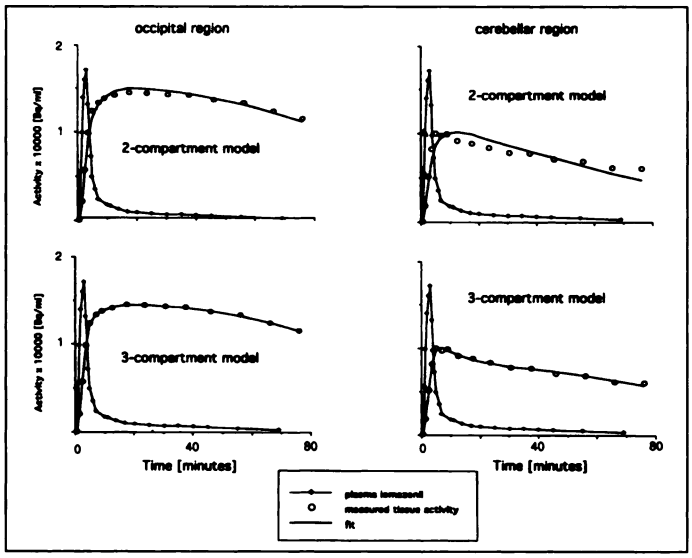

FIGURE 2. Tissue time-activity curves of an occipital and cerebellar region and fit with the two- and three-compartment models with no parameter constraints.

RESULTS

Specific activity ranged from 11 to 25 Ci/mmole. Receptor occupancy was estimated as follows: maximum uptake of [^{11}C] activity in the different regions was determined in (Bq/ml) and assumed to represent specific binding of iomazenil to receptors. Bmax in occipital cortex was assumed to be 160 n*M* (*12*). These assumptions yielded an estimate of occipital receptor occupancy ranging from 10% to 22%.

Figure 2 illustrates the improvement of the fit in occipital cortex and cerebellum with the three-compartment model (no parameter constraints) compared to the two-compartment model. In both regions, although more pronounced in the cerebellum, there is considerable bias in the fit with the two-compartment model which is completely removed by the three-compartment model.

Reduced chi square analysis (adjusted for degrees of freedom) as a measure of goodness-of-fit is shown for the different methods in the cerebellum and occipital cortex in Table 2. In all regions except the pons, F-test statistics demonstrated a highly significant reduction in the sum of squares ($p < 0.01$) for all methods using three compartments compared to the two-compartment model. Among the methods using the three-compartment model, there was still a significant difference between method B and method E, but not between methods C or D (constraining 1 parameter) and E (no parameter constraints).

Table 3 summarizes the fitting results for the receptor-related parameters derived from the different methods. In the receptor-poor regions pons and striatum, method C yielded physiologically meaningless values for k3′, k4, and subsequently DVs and K1/k2′ × k3′, in two subjects.

Table 4 demonstrates the values for the transport-related parameter K1, the nonspecific distribution volume DV′ and k4

TABLE 2
Goodness-of-fit in Occipital Cortex and Cerebellum

Region		Chi square (reduced) A	B	C	D	E
Cerebellum	Mean	1.64	0.36	0.32	0.27	0.20
	%COV	59	55	65	3	38
Occipital	Mean	0.57	0.32	0.27	0.27	0.25
	%COV	102	102	82	106	74

%COV = percentage coefficient of variation (s.d./mean × 100) among the five subjects.

TABLE 3
Estimates for Receptor-Related Parameters

Region		DV″	DVs	DVs	DVs	DVs	K1/k2′ × k3′				k3′			
		A	B	C	D	E	B	C	D	E	B	C	D	E
Cerebellum	Mean	13.3	10.8	11.6	9.5	10.7	0.56	0.48	0.47	0.41	0.16	0.14	0.10	0.09
	% COV sub	33.4	33.5	29.2	30.2	25.9	49.7	53.9	36.9	49.1	56.4	48.3	21.1	14.7
	% COV sim	3.7	6.2	9.4	5.5	30.4	8.4	14.6	4.3	21.4	11.0	14.2	4.2	27.9
Frontal	Mean	20.2	18.4	18.8	17.7	18.1	0.95	0.88	0.88	0.85	0.28	0.27	0.17	0.18
	% COV sub	24.9	24.9	27.7	28.4	32.3	41.6	29.6	35.7	30.5	46.1	24.0	21.3	13.7
	% COV sim	5.1	6.6	8.9	7.9	11.6	9.1	17.1	7.3	18.5	11.3	16.8	7.2	14.1
Occipital	Mean	25.7	23.8	24.4	22.0	22.7	1.22	1.26	1.05	1.16	0.36	0.37	0.19	0.20
	% COV sub	20.5	19.9	23.6	18.2	26.1	37.7	49.3	33.8	38.1	46.0	26.6	17.5	15.3
	% COV sim	5.9	6.7	9.1	6.8	14.3	10.0	16.4	6.3	26.5	11.8	16.5	3.5	31.5
Pons	Mean	3.7	2.6	1.46*	1.1	2.9	0.23	0.14*	0.24	0.24	0.11	0.03*	0.06	0.10
	% COV sub	91.7	89.0	148.1*	187.0	67.7	155.0	216.0*	155.0	154.3	88.0	209.5*	105.0	76.8
	% COV sim	3.5	34.1	217.2	89.2	12.9	38.2	56.4	89.9	14.1	46.3	64.4	89.9	21.3
Striatum	Mean	6.4	3.5	5.88*	4.7	4.7	0.18	0.19*	0.23	0.26	0.05	0.06*	0.05	0.10
	% COV sub	55.1	89.2	34.0*	56.8	63.4	102.0	92.8*	66.4	57.3	86.1	88.0*	30.6	29.8
	% COV sim	3.3	24.8	34.1	10.8	13.5	25.9	23.6	10.0	29.6	27.2	24.0	17.6	41.6
Temporal	Mean	20.3	19.0	19.5	16.6	17.0	0.88	0.88	0.78	0.80	0.30	0.30	0.13	0.13
	% COV sub	21.8	23.6	28.0	26.5	33.7	35.3	38.4	30.0	33.0	49.0	29.4	22.5	16.5
	% COV sim	5.2	7.0	8.2	8.5	18.6	10.5	15.3	7.6	28.2	12.9	14.9	7.4	28.9
Thalamus	Mean	8.6	6.1	6.3	6.6	6.8	0.31	0.34	0.33	0.38	0.09	0.10	0.08	0.10
	% COV sub	29.2	37.7	21.4	30.4	23.3	44.3	53.1	40.9	47.7	54.5	62.4	47.3	23.3
	% COV sim	3.3	7.7	12.4	5.5	15.2	9.5	17.1	4.7	17.5	12.1	16.8	7.5	23.5
High/Low		3.52	4.99	4.33	4.54	4.02	4.24	4.43	3.35	3.22	3.76	4.91	2.56	1.73

*Mean and % COV sub of only three subjects; in two subjects the values were physiologically meaningless.
Mean = mean values of the five subjects; % COV sub = percentage coefficient of variation (= s.d./mean × 100) among the five subjects; % COV sim = mean of the % COV derived from the Monte Carlo simulation in the five subjects; high/low = (occipital + frontal + temporal)/(pons + striatum + thalamus).
Values for DV are given in ml g^{-1}, K1/k2′ × k3′ in ml min^{-1} g^{-1} and k3′ in min^{-1}.

as calculated with the different methods. Also indicated is the coefficient of variation among the subjects (%COVsub) and the mean of the coefficient of variation determined in the Monte Carlo simulation (%COVsim).

The effect of shortening the study duration on parameters DV″ (two-compartment model) and k4 (three-compartment model, no parameter constraints) is demonstrated in Figure 3, upper panel. There is considerable underestimation of DV″ for study durations less than 100 min. This effect is due completely to the application of the over-simplified two-compartment model to data generated with the three-compartment model. The lower panel of Figure 3 demonstrates the identifiability of k4 as function of study duration. The result of 60 runs of a Monte Carlo simulation, in which tissue-time activity curves were generated with the three-compartment model (same parameters as in the left panel) and the addition of 10% pseudo-Gaussian noise is shown. The estimation of k4 becomes unstable for study durations less than 70 min. Accordingly, the estimation of the distribution volume DVs, which is critically dependent on k4, showed the same trend.

DISCUSSION

Specific Activity

To deduce information on receptor density from the kinetic analysis of binding data, it is important to estimate what fraction of the available receptors became occupied by the injected ligand. If that fraction is negligible, parameter k3 reflects the product of Bmax and kon. If considerable receptor occupancy occurs, however, the amount of receptors available for binding becomes time-dependent and k3 will be reduced. The specific activity of our iomazenil was relatively low and the estimation of receptor occupancy shows that receptor occupation in the range of 10%–20% may have occurred. It is therefore possible that the k3′ estimates and the parameter combinations related to it are underestimated by a similar amount. Such a systematic bias, however, should not severely affect the evaluation of the model alternatives and outcome measures for receptor density. The relative performance of the various methods tested can be evaluated through comparison of the parameter estimates presented in Tables 3 and 4.

Two-Compartment Versus Three-Compartment Model

Goodness-of-fit. Visual analysis of the fit in a cerebellar and an occipital region reveals evident bias in the fit with the two-compartment model (Fig. 2). Since the exchange of ligand between the nonspecific and specific compartments is faster in the areas with high receptor densities, these compartments tend to act kinetically more like one compartment in the receptor-rich areas. This explains why bias is more pronounced in the cerebellar rather than the occipital cortex. Evaluation of the goodness-of-fit by chi square analysis demonstrates the same result. The reduction in chi square when using the three-compartment model with no parameter constraints compared to the two-compartment model is more pronounced in the cerebellar than occipital cortex (90% versus 60% reduction, Table 2). The same tendency was also observed for flumazenil (*9*). This bias leads to an underestimation of K1 and DV values with the two-compartment model. The underestimation of DV″ values is not evident from the numbers in Table 3, since the distribution volume of the two-compartment model represents specific plus nonspecific binding, whereas DVs of the three-compartment model are assumed to reflect only specific binding. One can also calculate the distribution volume of total tissue binding with the three-compartment model [DVtot3comp = K1/k2′ (1 + k3′/k4)]. Linear regression yielded: DV″2comp

TABLE 4
Estimates of K1, DV′ and k4

Region		K1					DV′				k4			
		A	B	C	D	E	B	C	D	E	B	C	D	E
Cerebellum	Mean	0.29	0.37	0.38	0.35	0.36	3.55	3.36	4.34	4.59	0.051	0.041	0.050	0.040
	% COV sub	29.5	39.0	38.6	29.8	30.3	34.4	30.5	48.5	41.0	31.0	34.4	31.5	38.2
	% COV sim	2.6	4.3	4.4	4.3	8.0	4.2	3.2	5.0	10.3	8.8	21.0	4.5	33.6
Frontal	Mean	0.30	0.38	0.38	0.37	0.39	3.55	3.36	4.46	4.00	0.051	0.050	0.050	0.051
	% COV sub	26.5	30.7	34.2	35.2	40.0	34.4	30.5	31.0	40.4	31.0	30.6	31.5	31.5
	% COV sim	2.6	4.3	4.4	4.3	8.0	4.2	3.2	9.1	9.2	8.8	20.3	4.5	27.4
Occipital	Mean	0.34	0.42	0.43	0.38	0.41	3.55	3.36	5.77	5.58	0.051	0.053	0.050	0.059
	% COV sub	24.8	25.7	32.4	27.1	28.5	34.4	30.5	23.5	26.9	31.0	47.1	31.5	40.3
	% COV sim	2.7	4.6	5.0	3.7	6.6	4.2	3.2	5.6	23.8	8.8	20.1	4.5	38.9
Pons	Mean	0.23	0.32	0.22	0.19	0.32	3.55	3.36	3.21	1.52	0.051	0.020*	0.050	0.062
	% COV sub	41.3	45.0	53.5	41.0	35.9	34.4	30.5	43.1	71.9	31.0	154.1*	31.5	76.0
	% COV sim	3.4	9.0	5.2	3.5	8.7	4.2	3.2	3.5	11.8	8.8	20.1	4.5	18.9
Striatum	Mean	0.24	0.29	0.29	0.31	0.31	3.55	3.36	2.95	2.42	0.051	0.036*	0.050	0.060
	% COV sub	31.3	40.0	38.5	33.2	34.1	34.4	30.5	35.6	38.1	31.0	94.6*	31.5	31.3
	% COV sim	3.0	3.8	4.2	5.1	6.0	4.2	3.2	8.4	11.9	8.8	122.1	4.5	35.4
Temporal	Mean	0.28	0.35	0.36	0.32	0.32	3.55	3.36	5.79	5.90	0.051	0.048	0.050	0.058
	% COV sub	23.4	27.1	31.7	25.1	26.4	34.4	30.5	16.8	16.2	31.0	46.7	31.5	46.3
	% COV sim	2.5	4.4	4.8	3.7	7.5	4.2	3.2	9.2	9.0	8.8	19.1	4.5	45.5
Thalamus	Mean	0.29	0.39	0.38	0.47	0.42	3.55	3.36	3.19	2.68	0.051	0.051	0.050	0.057
	% COV sub	34.9	46.7	41.2	67.0	44.7	34.4	30.5	65.8	43.2	31.0	45.2	31.5	32.3
	% COV sim	2.9	4.6	4.3	5.2	6.9	4.2	3.2	6.3	10.0	8.8	24.4	4.5	24.3

*Mean and % COV sub of only three subjects; in two subjects, the values were physiologically meaningless.
Values for K1 are given in ml min^{-1} g^{-1} and k4 in min^{-1}.

= 0.90 DVtot3comp − 0.11, r = 0.99 (all regions, all subjects), which demonstrated a 10% underestimation of DV with the two-compartment model.

Parameter Identifiability. The coefficient of variation calculated with the Monte Carlo simulation ranged from 2.5%–3.4% for K1 and 3.3%–5.9% for DV″. These values are clearly the lowest of all methods, thereby demonstrating that the two-compartment model yields the most stable estimates of K1 and DV″.

Estimates of Kinetic Parameters Versus Scan Duration. The underestimation of DV″ is furthermore dependent on scan duration, as DV″ underestimation gets progressively more pronounced in scans of less than 100 min (Fig. 3, upper panel). This is in agreement with results from experiments in monkeys that demonstrated similar underestimation in scans of less than 120 min (*16*).

With the three-compartment model, the critical parameter with regard to identifiability turned out to be k4 (Figure 3, lower panel). With less than 70 min of data, the coefficient of variation increased remarkably. With SPECT and the same model, an overestimation of the binding potential was demonstrated for scan durations less than 50–60 min (*12*).

All these considerations indicate that the two-compartment model is not complex enough to accurately reflect the kinetics of iomazenil, even in the areas with high receptor density. This is in contrast to flumazenil, where the two-compartment model was sufficient to describe the kinetics, except in areas with very low receptor densities (*9*). That difference is probably due to the considerably higher dissociation rate k4 of flumazenil (0.12–0.41 versus 0.04–0.06 min^{-1}) that allows a faster exchange of ligand between the nonspecific and specific compartments. The longer minimal scan duration required to obtain stable DV″ values is a further disadvantage of the two-compartment model. Based on these observations, the two-compartment model is considered less suitable to derive accurate receptor estimates than a three-compartment configuration.

Three-Compartment Models

For the transport parameter K1 identifiability is somewhat better for the models with parameter constraints compared to the full three-compartment model (%COV 4.3%–4.4%, for methods B–D versus 8% for method E, Monte Carlo simulation).

Range of Receptor-Related Parameters. The range of receptor related parameters K1/k2 × k3′ is compressed with method D and E, of parameter k3′ with methods B, D and E (ratio of DVshigh/DVslow <3). Based on this observation, these combinations of parameters and methods seem unsuitable for the estimation of benzodiazepine receptor density and are not further discussed. For the remaining combinations the ratio ranges from 4.02%–4.99%.

Identifiability of Parameter Estimates. Of the combinations of parameters and methods with a range >4, parameter DVs displays a smaller coefficient of variation than K1/k2 × k3′ or k3′. For DVs the methods with parameter constraints show less variability in all regions, except in the pons and the striatum, than method E, which had no parameter constraints. Method C, which constrains the nonspecific distribution volume DV′ to a common value, shows an exceedingly high coefficient of variation of 217% in the pons. In two subjects the method yielded even physiologically meaningless values for DVs. A likely explanation was previously described.

In the areas with medium-to-high receptor densities, DVs estimated with methods B and D show a lower coefficient of variation compared to method C. Based on this finding, and the earlier observation that the range of DVs is higher than the one of k3′ and K1/k2′ k3′, DVs values derived from methods B and D are considered to yield the most accurate estimates for receptor densities.

Goodness-of-fit. Among the three-compartment configurations, there is still a small but significant (F-test) difference between methods B and E, but not among methods C, D and E.

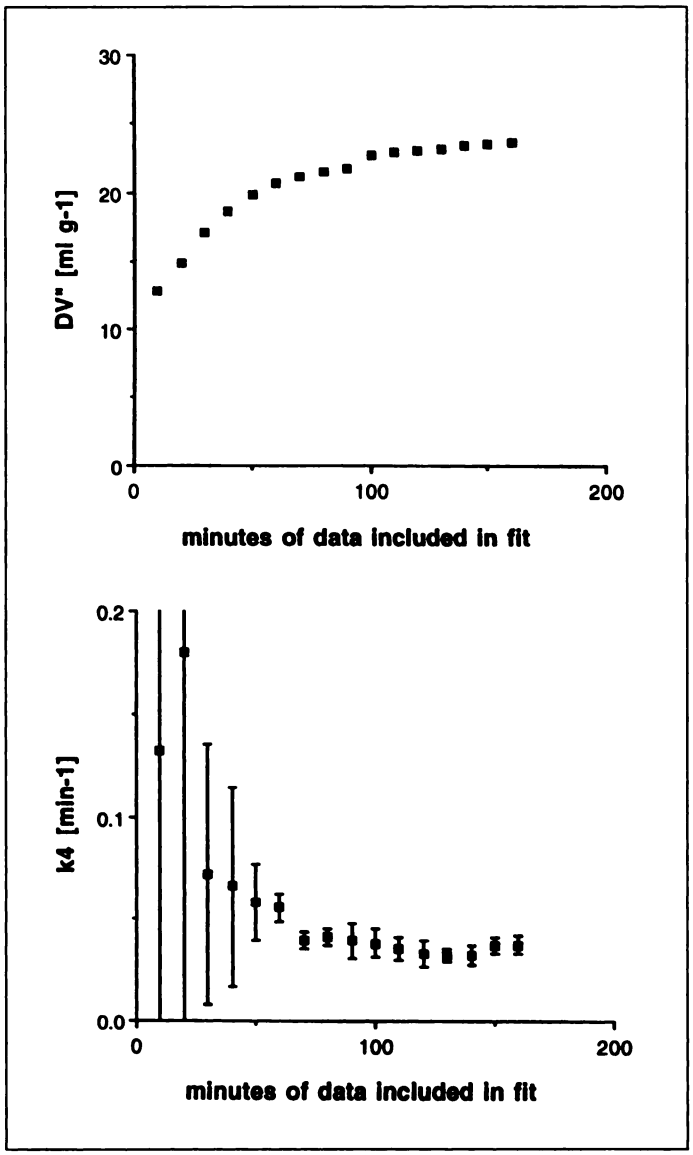

FIGURE 3. Stability of model derived parameters versus study duration. (Top) DV" values calculated with the two-compartment model from a simulated tissue time-activity curve generated with the three-compartment model (K1 = 0.41, k2 = 0.09, k3 = 0.16, k4 = 0.03). (Bottom) Mean and s.d. of k4 calculated with the three-compartment model versus scan duration derived from a Monte Carlo simulation.

Estimation of the Nonspecific Distribution Volume (DV')

On physiological grounds, regional differences in nonspecific binding can be assumed to be minimal. With method E and somewhat less with method D, however, there is a considerable range of values (1.52–5.58 for method E, and 3.21–5.77 for method D). Some of this variation may be explained by distortion effects due to the limited spatial resolution of the PET scanner. These effects lead to a underestimation of the true count density in smaller structures which is mathematically reflected in a reduction of K1 and, subsequently, K1-related parameter combinations such as the distribution volume. This explanation is supported by the regional distribution of the K1 values (Table 4) which are lowest in the small structures of the pons and the striatum. The degree of variation in DV′ determined with method E, however, is considerably larger than for K1, indicating that other effects also contribute to this variation. Constraining DV′ not only removes this variation but also seems to yield physiologically reasonable values. The ratio of specific to nonspecific binding (DVs/DV′) in occipital cortex is 6.7, 6.5 and 4.1 for methods B, C and E, respectively. Displacement experiments with flumazenil have shown that approximately 13% of total binding of iomazenil is nonreplaceable in cortical regions (*12*). This yields a DVs-to-DV′ ratio of 6.7, which is in excellent agreement with the ratio determined with methods B and C. Identifiability of DV′ is also clearly improved with these methods as is demonstrated by the smaller coefficient of variation. In two subjects, however, method C did not yield reasonable values for k3′, k4 and subsequently DVs. A likely explanation is discussed later.

Estimation of k4

Using the three-compartment model with no parameter constraints, the dissociation rate k4 displays the lowest identifiability of the presented parameters with the coefficient of variation (Monte Carlo simulation), ranging from 18.9% to 45%. Identifiability is considerably improved by the methods that estimate a common value for k4 (8.8% for method B, 4.5% for method D). With the full three-compartment model, the value for k4 ranged from 0.04–0.06 min^{-1}; both methods with a common k4 yielded a value of 0.05 min^{-1}. These values are higher than those reported by Abi-Dhargam et al. (*12*) in their SPECT study (0.014–0.034 min^{-1}). The reason for this discrepancy is not clear.

Coupling of Multiple Regions by Common Parameters

Constraining parameters is a common method to improve the reliability of parameters estimated with models of higher complexity (*9,17*). It is based on the assumption that certain physiological properties such as nonspecific binding do not vary among the ROIs substantially. A common approach is to estimate the nonspecific distribution volume (K1/k2′) in a region devoid of receptors and then fix this parameter in receptor-rich regions. A problem with this approach, however, arises when there are no regions with sufficiently low receptor density, as may be the case with benzodiazepine receptors. Even the pons, which is sometimes used as a receptor-poor region, displays a considerable amount of specific binding (*12*). Another potential problem might be that any error in the parameter estimates made in the reference region will propagate through all subsequent fits. The approach chosen in this study to constrain parameters does not require a reference region devoid of receptors. By simultaneous fitting data from all regions with coupling of the supposedly constant parameters, the amount of available data is substantially increased. The procedure was first applied to the estimation of metabolic parameters in cardiac PET studies with ^{11}C-acetate (*13*). The method is highly successful in increasing the identifiability of parameters, a phenomenon which is also demonstrated by the reduction of the coefficient of variation in Tables 2 and 3. Furthermore, it is not sensitive to errors made in individual regions. Caution is warranted, however, when choosing which parameters to couple. The common values of the coupled parameters are in a way an average of several regional values and will therefore be larger than the ones calculated with no parameter constraints in some individual regions and smaller in others. With DV′ this may lead to identifiability problems. If the coupled values are still smaller than the total distribution volume as determined with no parameter constraints, k3′ will be decreased and DVs values, being proportional to the product of DV′ and k3′, will still be stable. If, however, the coupled DV′ becomes equal or even larger than the total distribution volume calculated with no constraints, k3′, k4 and DVs lose all physiological meaning. This problem was encountered in the pons and the striatum of two subjects, where the coupling of only DV′ (method C) led to physiologically unreasonable values for the receptor-related

parameters. This problem was avoided by coupling only k4 and, somewhat surprisingly, by coupling DV′ and k4. Parameter k4 seems an ideal candidate for coupling. There is good physiological evidence to assume that it does not vary much across regions. Because it is independent of K1, it will not be affected by distortion effects.

CONCLUSION

Quantitative receptor imaging with a single bolus injection of iomazenil and PET is best performed with a three-compartment model including parameter constraints. In the present study, the most reliable measure for receptor density was DVs, calculated by constraining k4 or both k4 and K1/k2′. The applied method to constrain parameters (simultaneous fitting of data from multiple brain regions coupled by common parameters) proved to be effective in increasing the identifiability of parameter estimates. It does not require a region devoid of receptors, but warrants careful selection of the parameters to be coupled.

ACKNOWLEDGMENTS

The authors thank K. Leenders, P. Maguire and A. Antonini for their technical assistance and I. Eberle for the synthesis of the [^{11}C]iomazenil.

REFERENCES

1. Bartenstein P, Ludolph A, Schober O, et al. Benzodiazepine receptors and cerebral blood flow in partial epilepsy. *Eur J Nucl Med* 1991;18:111–118.
2. Cordes M, Henkes H, Ferstl F, et al. Evaluation of focal epilepsy: a SPECT scanning comparison of ^{123}I-iomazenil versus HMPAO. *Am J Neuroradiol* 1992;13:249–253.
3. Ferstl FJ, Cordes M, Cordes I, et al. Iodine-123-iomazenil SPECT in patients with focal epilepsies—a comparative study with ^{99m}Tc-HMPAO SPECT, CT and MRI. *Adv Exp Med Biol* 1991;287:405–412.
4. Savic I, Roland P, Sedvall G, et al. In vivo demonstration of reduced benzodiazepine receptor binding in human epileptic foci. *Lancet* 1988;2:863–866.
5. Schubiger PA, Hasler PH, Beer WH, et al. Evaluation of a multicentre study with iomazenil—a benzodiazepine receptor ligand. *Nucl Med Commun* 1991;12:569–582.
6. Venz S, Cordes M, Schmitz B, et al. Iodine-123-iomazenil- and ^{99m}Tc-HMPAO in the diagnosis of focal epilepsies: a comparison of untreated and treated patients. *Nuklearmedizin* 1994;33:1–7.
7. Price JC, Sadzot B, Mayberg HS, et al. Quantification of human benzodiazepine receptor concentration using ^{11}C Ro-15-1788, PET and tracer kinetic modeling. *J Nucl Med* 1990;31:709–714.
8. Persson A, Ehrin E, Eriksson L, et al. Imaging of ^{11}C-labeled RO-15-1788 binding to benzodiazepine receptors in the human brain by PET. *J Psychiatr Res* 1985;19:609–622.
9. Koeppe RA, Holthoff VA, Frey KA, Kilbourn MR, Kuhl DE. Compartmental analysis of [^{11}C]flumazenil kinetics for the estimation of ligand transport rate and receptor distribution using PET. *J Cereb Blood Flow Metab* 1991;11:735–744.
10. Laruelle M, Abi-Dargham A, et al. SPECT quantification of [^{123}I]iomazenil binding to benzodiazepine receptors in nonhuman primates. II. Equilibrium analysis of constant infusion experiments and correlation with in vitro parameters. *J Cereb Blood Flow Metab* 1994;14:453–465.
11. Innis R, Zoghbi S, Johnson E, et al. SPECT imaging of the benzodiazepine receptor in non-human primate brain with ^{123}I-Ro-16-0154. *Eur J Pharmacol* 1991;193:249–252.
12. Abi-Dargham A, Laruelle M, Seibyl J, et al. SPECT measurement of benzodiazepine receptors in human brain with iodine-123-iomazenil: kinetic and equilibrium paradigms. *J Nucl Med* 1994;35:228–238.
13. Raylman RR, Hutchins GD, Beanlands RSB, Schwaiger M. Modeling of carbon-11-acetate kinetics by simultaneously fitting data from multiple ROIs coupled by common parameters. *J Nucl Med* 1994;35:1286–1291.
14. Mintun MA, Raichle ME, Kilbourn MR, et al. A quantitative model for the in vivo assessment of drug binding sites with PET. *Ann Neurol* 1984;15:217–227.
15. Westera G, Eberle I, Hunkeler W, et al. The production of [^{11}C]iomazenil. *J Lab Compd Radiopharm* 1993;32:169–170.
16. Laruelle M, Baldwin RM, Rattner Z, et al. SPECT quantification of [^{123}I]iomazenil binding to benzodiazepine receptors in nonhuman primates. I. Kinetic modeling of single bolus experiments. *J Cereb Blood Flow Metab* 1994;14:439–452.
17. Frost JJ, Douglass KH, Mayberg HS. Multicompartmental analysis of ^{11}C-carfentanil binding to opiate receptors in humans measured with PET. *J Cereb Blood Flow Metab* 1989;9:398–409.